Estimating nonlinearities in twophase flow in porous media.

Jianfeng Zhang, Guy Chavent, Jérôme Jaffré

INSTITUT NATIONAL DE RECHERCHE EN INFORMATIQUE ET EN AUTOMATIQUE

Estimating nonlinearities in twophase flow in porous media

Jianfeng Zhang — Guy Chavent — Jérôme Jaffré

N° 6892

Mars 2009

Thème NUM

ISSN 0249-6399 ISRN INRIA/RR--6892--FR+ENG

INSTITUT NATIONAL
DE RECHERCHE
EN INFORMATIQUE
ET EN AUTOMATIQUE

INRIA

centre de recherche
PARIS - ROCQUENCOURT

Estimating nonlinearities in twophase flow in porous media

Jianfeng Zhang* , Guy Chavent†* , Jérôme Jaffré*

Thème NUM — Systèmes numériques
Équipes-Projets Estime

Rapport de recherche n° 6892 — Mars 2009 — 23 pages

Abstract: In order to analyze numerically inverse problems several techniques based on linear and nonlinear stability analysis are presented. These techniques are illustrated on the problem of estimating mobilities and capillary pressure in one-dimensional two-phase displacements in porous media that are performed in laboratories. This is an example of the problem of estimating nonlinear coefficients in a system of nonlinear partial differential equations.

Key-words: flow in porous media, inverse problem, estimation of nonlinear coefficients.

* INRIA, Domaine de Voluceau, 78153 Le Chesnay Cedex, France
† CEREMADE, Université Paris-Dauphine, France

Centre de recherche INRIA Paris – Rocquencourt
Domaine de Voluceau, Rocquencourt, BP 105, 78153 Le Chesnay Cedex
Téléphone : +33 1 39 63 55 11 — Télécopie : +33 1 39 63 53 30

Estimation des non-linéarités pour des écoulements diphasiques en milieu poreux

Résumé : Afin d'analyser numériquement des problèmes inverses on présente plusieurs techniques basées sur l'analyse de stabilité linéaire et non-linéaire. Ces techniques sont présentées pour le problème d'estimation des mobilités et de la pression capillaire dans des déplacements diphasiques unidimensionnels en milieu poreux réalisés en laboratoire. C'est un exemple de problème d'estimation des coefficients non-linéaires dans un système d'équations aux dérivées partielles non-linéaires.

Mots-clés : écoulement en milieu poreux, problème inverse, estimation des coefficients non-linéaires

1 Introduction

Multiphase flow in porous media is modelled by a set of nonlinear partial differential equations equations and it provides a very good practical example for the inverse problem of estimating nonlinear coefficients in nonlinear partial differential equations. The standard problem in petroleum engineering is to estimate the relative permeabilities and capillary pressure curves from laboratory experiments which consists of displacing a resident phase by injecting the other [16, 12, 13, 35, 26, 3, 5, 30]. The relative permeabilities and the capillary pressure are functions of the saturation of one of the phases. More recently experiments where the displacement is due to centrifugation were designed in order to improve the estimation of the capillary pressure function [6, 34, 31, 11]. Three-phase flow were also considered in [15, 28]. In this case the relative permeabilities and the capillary pressure are functions of two variables. In hydrogeology the Richards equation is often used and the problem of estimating its coefficients is considered in [22, 1].

Without trying to give a complete review we can add to this bibliography several interesting contributions [17, 33, 21, 20] and two reviews for parameter estimation in multiphase flow [18, 32].

In this paper we present several ingredients for a successful numerical estimation of the relative permeabilities and the capillary pressure. In Section 2 we introduce the mathematical model for two-phase flow and in Section 3 we set the parameter estimation problem as a minimization problem. Multiscale parameterization is adressed in Section 4. Some linear analysis of the problem is presented in Section 5 and confidence intervals are calculated in Section 6 using edgehog extremal solutions. Techniques for nonlinear analysis are presented in Section 7 and implemented numerically in Section 8.

2 A model for a two-phase displacement in porous media

In several laboratories core samples collected from oil fields are analyzed to determine their flow properties. A typical experiment consist in displacing a resident wetting fluid (subscript w), say water, by a nonwetting fluid (subscript nw), say oil. The displacement may be driven by injecting the nonwetting fluid through one extremity of the core or by centrifugal forces. These experiments are sketched in Fig. 1.

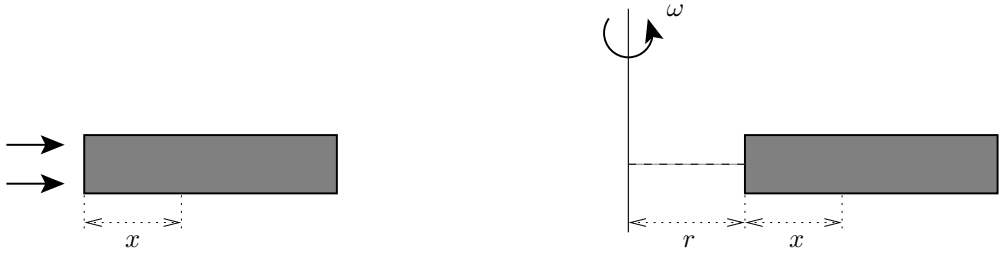

Figure 1: Two-phase displacement by injection (right) or by centrifugation (left)

Two-phase displacement is governed by a generalized Darcy's law and, in laboratory experiments, it is usually assumed to be incompressible and one-dimensional. Using the global pressure formulation [14] the displacement is modelled by the following nonlinear equation :

$$\begin{aligned} &\phi\frac{\partial S}{\partial t} + \frac{\partial q_w}{\partial x} = 0, \\ &q_w = -Ka(S)\frac{\partial S}{\partial x} + q_T(t)b_T(S) + q_G b_G(S), \end{aligned} \tag{1}$$

where $S = S_w((0 \leq S \leq 1)$ is the saturation of the wetting fluid, q_w its Darcy velocity, ϕ is the porosity of the rock and K is its absolute permeability. The total flow rate $q_T = q_w + q_{nw}$ is the sum of the flow rate of the two phases and is given by

$$q_T = -Kd(S)[\frac{\partial P}{\partial x} - \rho(S)H]. \tag{2}$$

The global pressure P [14] is given by

$$P = \frac{1}{2}(p_w + p_{nw}) + \gamma(S), \tag{3}$$

with p_w, p_nw the phase pressures and γ defined below.

H is a gravity or centrifugation function. In case of a standard displacement $H(x) = g\nabla Z(x)$ where g is the Newton constant and Z is the depth at the location x. In case of a displacement by centrifugation $H(x) = \omega^2(r + x)$ where ω is the angular speed, r is the distance from the rotation axis to the closest extremity of the core (see Fig. 1). The total flow rate q_T is independent of x because of the incompressibility assumption.

The gravity or centrifugation field q_G is given by

$$q_G = K\frac{\rho_w + \rho_{nw}}{2} H \tag{4}$$

where ρ_w and ρ_{nw} are the densities of the wetting fluid and the nonwetting fluid respectively.

We have introduced above the coefficients a, b_T, b_G, d, ρ, γ which are functions of the saturation S. They relate to the relative permeability functions kr_w and kr_{nw} and to the capillary pressure function $p_c = p_w - p_{nw}$ through the following relations :

$$a = \frac{k_w k_{nw}}{k_w + k_{nw}} p_c', \qquad b_T = \frac{k_w}{k_w + k_{nw}}, \qquad b_G = \frac{k_w k_{nw}}{k_w + k_{nw}} \frac{\rho_w - \rho_{nw}}{\frac{1}{2}(\rho_w + \rho_{nw})},$$

$$d = k_w + k_{nw}, \qquad \rho = \frac{k_w\rho_w + k_{nw}\rho_{nw}}{k_w + k_{nw}}, \quad \gamma = \int_0^S (b_T(s) - \frac{1}{2})\frac{dp_c}{dS},$$

$$k_i = \frac{kr_i}{\mu_i},\ i = w, nw.$$

where $\mu_i, i = w, nw$ are the viscosities of the two phases.

The relative permeabilities kr_w and kr_{nw} and the capillary pressure p_c are functions of the saturation which satisfy the following physical properties :

$$\begin{aligned} &kr_w \geq 0,\ kr_w \text{ increasing},\ \ kr_{nw} \geq 0,\ kr_{nw} \text{ decreasing},\ \ kr_w(0) = kr_{nw}(1) = 0, \\ &p_c \geq 0,\ p_c \text{ decreasing}. \end{aligned} \tag{5}$$

To equations (1), (2) we add various boundary conditions depending on the experiments [36].

3 The parameter estimation problem

The problem is to estimate relative permeabilities and pressure capillary functions. For this purpose experiments are set up so the following measurements are available :

1. Local measurements : saturations $S^m_{k,i}$ are measured at different times t_k and different locations x_i;
2. Global measurements : cumulated productions $Q^m_k = \int_0^{t_k} \phi_w(t)dt$ and pressure drops ΔP_k are measured at different times t_k.

The problem of estimating the mobility and pressure capillary functions is set as the problem of minimizing the error function J :

$$J(kr_w, kr_{nw}, p_c) = \sum_k \sum_i w_s^{k,i}(S^c_{k,i} - S^m_{k,i})^2 + \sum_k w_q^k(Q^c_k - Q^m_k)^2 + \sum_k w_p^k(\Delta P^c_k - \Delta P^m_k)^2. \tag{6}$$

Here the superscripts m and c refer respectively to "measured" and "calculated", and $w_s^{k,i}$, w_q^k and w_p^k are weights given to the measurements. The function J measures the difference between the measured quantities and that calculated with the model using the parameters kr_w, kr_{nw}, p_c.

The choice of parameterization of kr_w, kr_{nw}, p_c will be discussed in the next section and is crucial for a successful estimation. If computational costs are taken into account, the choice of the parameterization determines also the choice of the minimization method. If the choice of the parameterization gives a small number of parameters, say smaller than 15, then Levenberg-Marquart or trust region methods [29] can be used and be cost efficient. However, when the number of parameters becomes large, then these optimization methods become too expensive and quasi-Newton methods [2] using the gradient of J calculated with the adjoint method [7, 32] becomes the right choice. The drawback of this method is the difficulty to calculate the gradient and to implement this calculation. Therefore techniques of automatic differentiation were developped [25, 19] and sophisticated software like Tapenade and Adifor are now available.

Now we introduce some notations. We denote by $\mathcal{A}$ the set of admissible parameters $p = (kr_w, kr_{nw}, p_c)$, that is parameters that satisfy properties (5). $\mathcal{A}$ is a subset of a set $\mathcal{U}$. The direct mapping is the mapping φ

$$\begin{array}{rccc} \varphi: & \mathcal{A} \subset \mathcal{U} & \longmapsto & \mathcal{O} \\ & p = (kr_w, kr_{nw}, p_c) & \longmapsto & \varphi(p) = \varphi(u(p)) = (S^c, Q^c, \Delta P^c) \end{array} \tag{7}$$

which maps $\mathcal{A}$ into the Hilbert space $\mathcal{O}$ of observations. To solve the direct problem is to calculate $\varphi(p)$ for a given parameter p. This includes solving equations (1), (2) with appropriate initial and boundary conditions.

Let measurements $z = (Q^m, S^m, \Delta P^m)$ be given and let us write the error function J defined in (6) in compact form as

$$J(p) = \| \varphi(p) - z \|_W^2, \tag{8}$$

where $\| . \|_W$ is the weighted norm for $\mathcal{O}$ with W the diagonal matrix of the weights given to the various measurements. The inverse problem is to minimize J over the set of admissible parameters:

$$\text{Find } \hat{p} \in \mathcal{A} \text{ such that } J(\hat{p}) = \min_{p \in \mathcal{A}} J(p). \tag{9}$$

Of course in real life J does not vanish at the minimum because of errors in the model and in the measurements.

Several questions should be adressed. Is the minimum unique ? Are there local minima ? Is $\hat{p}$ very sensitive to uncertainties in the measurements z ? In the next sections we shall present several tools that are useful to answer these questions. They are based on linear analysis (Sections 5 and 6) and nonlinear analysis (Sections 7 and 8) of stability.

But, before, let us consider the question of parameterization, always crucial in parameter estimation.

4 Parameterization

A very common choice for parameterization of the relative permeabilities and capillary pressure is to use an analytical representation:

$$\begin{array}{l} k_w(S) = a_w S^{bw}, k_{nw}(S) = a_{nw}(1-S)^{bnw}, \\ \dfrac{dP_c}{dS} = c_0 + c_1 S + c_2 S^2, \ P_c(1.) = 0. \end{array}$$

The set of parameters to estimate is $p = (a_w, b_w, a_{nw}, b_{nw}, c_0, c_1, c_2)$, a set of 7 parameters. With such a choice it is usually not difficult to find a minimum to the minimization problem (8),(9).

However there are many cases for which such a representation is not suitable and the relative permeability and capillary curves do not have such analytical shapes. To do without such a priori shapes a possibility is to use a discrete representation of kr_w, kr_{nw}, P_c: $p = (k_{rwj}, j =$

$1, k_{rnwj}, P_{cj}, j = 1, \ldots, n_s)$ where $k_{rwj}, j = 1, k_{rnwj}, P_{cj}$ are the values of kr_w, kr_{nw}, P_c at a set of n_s discretization points of the saturation interval (0,1). Between these points the functions are linearly interpolated. Note that if one uses $n_s = 10$ equidistant saturation points, which is reasonable to capture nonstandard shapes, then the number of parameters is already 30.

As reported in [3] for a standard displacement experiment, it was possible to estimate the relative permeability curves using cumulated production, pressure drop and saturation measurements. However, without saturation measurement, the calculated optimal parameters were depending on the initial guess of the minimization algorithm. But when trying to estimate simultaneously relative permeability and capillary pressure curves, the minimization algorithm would usually get stuck in a local minimum with no practical interest.

This is the reason for the introduction of multiscale parameterization. The main idea is to adapt the parameterization as the minimization advances, starting with few parameters in order to estimate the main features of the functions, and increasing slowly their number to estimate their refined features. A simple example of a multiscale basis to expand a function is the Haar basis as represented in Fig. 2.

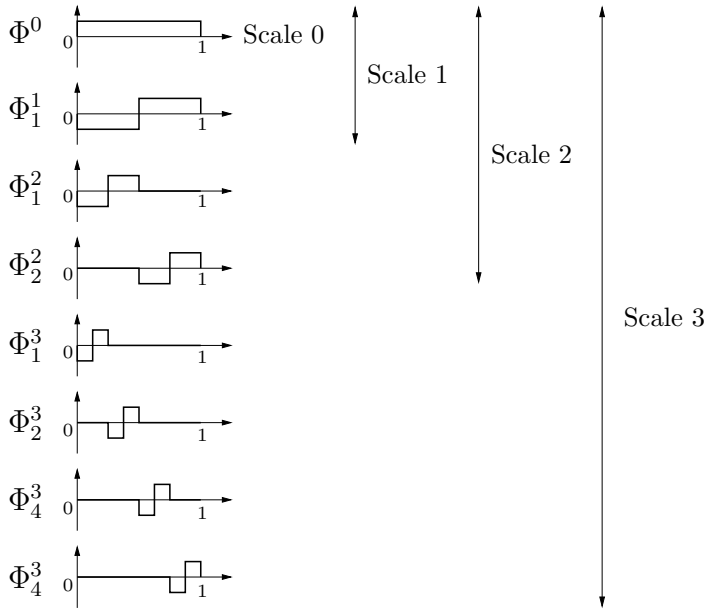

Figure 2: The Haar basis

In practice one endpoint of each of the relative permeability and capillary curves is known, so the continuous piecewise linear representation of the functions are uniquely defined by their piecewise constant derivatives which will be parameterized with the Haar basis :

$$\frac{dk_{rw}(S)}{dS} = (c_r w)^0 \Phi^0(S) + \sum_{i=1}^{n_s-1} \sum_{j=1}^{2^{i-1}} (c_r w)^i_j \Phi^i_j(S),$$

and similarly for $\frac{dk_{rnw}(S)}{dS}, \frac{dP_c(S)}{dS}$. Note that with such a parameterization enforcing conditions (5) is simple.

Then a multiscale optimization proceeds as follows:

1. Minimize at scale $i = 0$.
2. Augment i by 1.

3. Minimize at scale i using as starting point functions obtained by linearly interpolating that estimated with scale $i-1$.

4. If $i \geq i_{\max}$ or if scales $i-1$ and i give the same estimated function, stop.
   If not go to 2.

With such a procedure, the simultaneous estimation of relative permeability and capilary curves was successful while it failed when using a standard discrete parameterization [3]. Fig. 3 shows the progression of the multiscale parameterization for relative permeabilities and capillary pressure.

An important advantage of multiscale optimization is that it is adaptive. It does not require to fix a priori the number of parameters which increases as the number of steps of multiscale optimization increases until the difference between two scales is not anymore significant. Therefore the multiscale optimization procedure determines itself an almost optimal number of parameters necessary to interpret the available data.

5 Stability analysis based on the Hessian

In this section we show how to obtain some information concerning the inverse problem using the Hessian of J. We linearize φ around a given parameter p_0. Let us perturbate p_0 into p with a small perturbation $\delta p = p - p_0$. Taylor's expansion gives

$$\varphi(p) \approx \varphi(p_0) + \varphi'(p_0)\delta p.$$

If we introduce $\delta z = z - \varphi(p_0)$, the observation error function can actually be written as a quadratic function of δp :

$$J(\delta p) = \| \varphi'(p_0)\delta p - \delta z\|^2_W. \tag{10}$$

Then the inverse problem is to minimize this function and the minimum $\delta\hat{p}$ satisfies

$$H\delta\hat{p} = \varphi'(p_0)^t W \delta z \tag{11}$$

with $H = \varphi'(p_0)^t W \varphi'(p_0)$ the Hessian. We note that the matrix $\varphi'(p_0)$, which is the jacobian matrix of φ at p_0, can be viewed as the sensitivity matrix for φ.

Therefore solving the linearized inverse problem reduces to solving the linear system (11) and this explains the importance of studying the Hessian H.

To illustrate this we shall consider three problems of parameter estimation for which, from realistic data obtained in centrifugal experiments [6], we generated the measured observations with our simulation code. These problems are :

1. estimating relative permeabilities while measuring saturation profiles,

2. estimating relative permeabilities while measuring productions,

3. estimating relative permeabilities and capillary pressure while measuring saturation profiles.

The aim of this analysis is to study the importance of the choice of measurements for estimating kr_w, kr_{nw}, p_c.

Numerical results for these three problems are presented respectively in figures 4, 5 and 6. On each figure the parameters (before and after optimization and exact) and the observations (measured and calculated after optimization) are shown. The relatives permeabilities and the capillary pressure were discretized using the multiscale parameterization discussed in Section 4 with thirty parameters for each function. The saturation were observed at 6 different times in 15 locations to give the saturation profiles which are presented. The production of the displaced fluid (the nonwetting fluid) was observed at the same 6 different times as the saturation profiles.

In Figures 4, 5 and 6 the Hessian is also represented as a function of two variables which are the indices of the parameters to be estimated. They are ordered so that corresponding to the mobility of the wetting fluid, that corresponding to the mobility of the nonwetting fluid and that

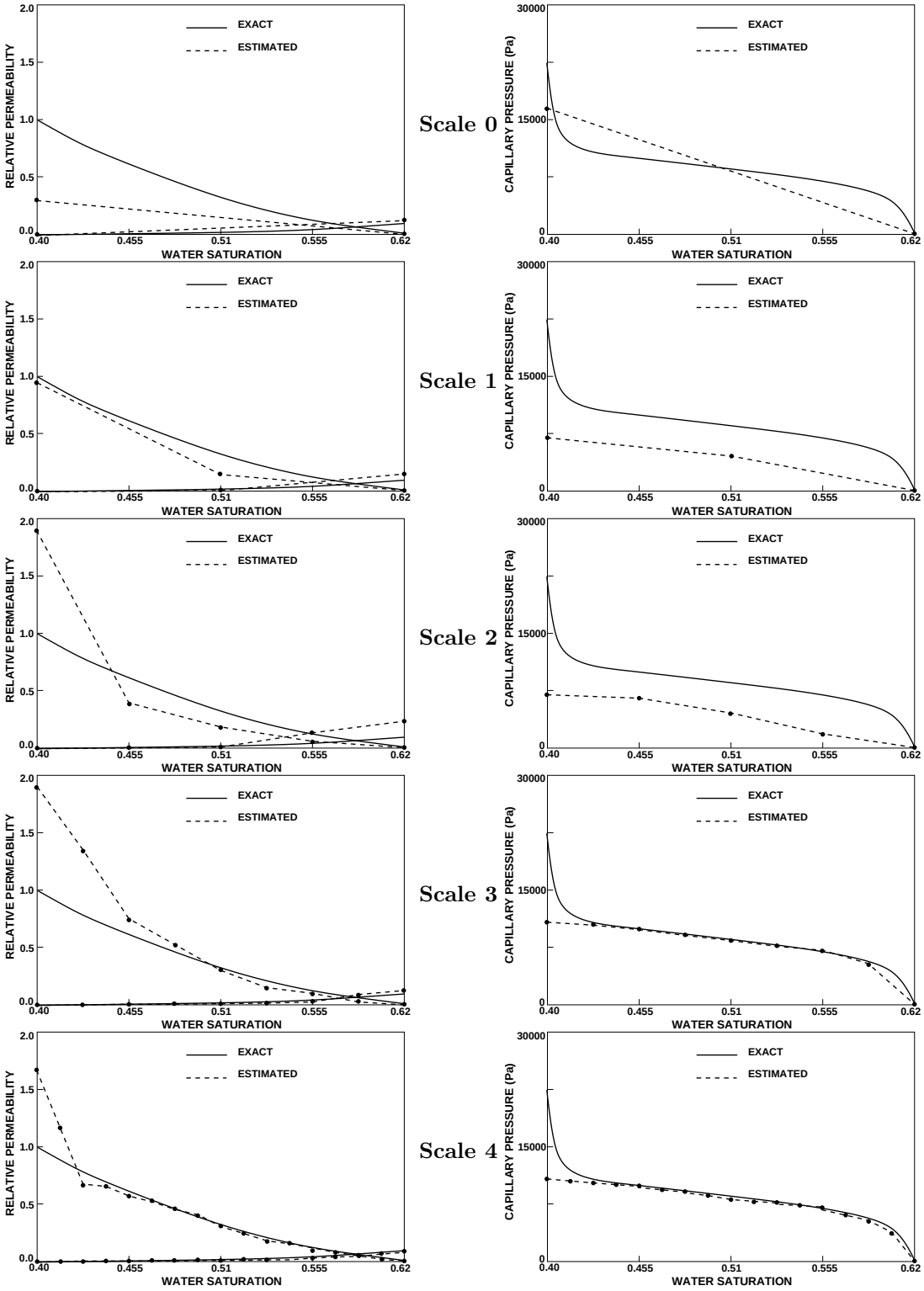

Figure 3: Relative permeability and capillary pressure curves estimated with multiscale parameterization

corresponding to the capillary pressure are in this order. For the two first experiments the singular values of the Hessian are also shown. Finally we drew the sensitivity of the obervations to the parameters that we calculated as the norms of the vector columnns of the Jacobian $\varphi\prime(p_0)$, each columnn corresponding to the derivative of φ with respect to a parameter.

We first observe that the parameters corresponding to small values of the saturation (smaller than 0.4) are not well estimated. This is not surprising since during the simulation these saturation are not reached (see saturation profiles). Therefore the error function is not sensitive to these parameters and the inverse problems is ill-posed. This is confirmed by the shape of the Hessian which have many coefficients which are very small and by its many zero singular values. Actually the direct mapping φ itself is not sensitive to these parameters as the sensitivity of the observations to these coefficients is zero.

However we may notice differences between Problems 1 and 2 (observing saturation profiles versus observing productions). The parameter estimation works better for Problem 1 : the estimated mobilities are closer to the exact ones. Another way to look at this is to compare the singular values of the Hessian for the two problems. We see that Problem 1 has fewer zero singular values of the Hessian so it is better conditionned.

Still comparing Problems 1 and 2 we observe that the Hessian in Problem 1 is more concentrated along the diagonal. This indicates that for this problem the parameters are less coupled which is a definitive advantage when minimizing.

These comparisons between Problems 1 and 2 give an answer to a practical question. It is more complicated to measure saturation profiles than it is to measure production, so are these efforts useful ? By analyzing the Hessian the answer is yes, and this is confirmed by numerical experiments [3, 4, 6].

Finally, considering Problem 3, we observe that the saturation profiles is more sensitive to the capillary pressure than to mobilities. This is a confirmation of the intuition of engineers which designed these centrifugation experiments in order to improve the estimation of capillary pressure.

Observation of Hessian H

- The residual is not sensitive to parameters corresponding to small coefficients of H.
- If H close to diagonal form, parameters are uncoupled and optimization is easier.
- The more singular values are nonzeros, the better the conditionnement of the optimization problem is.

6 Calculation of confidence intervals using edgehog extremal solutions

There is a large litterature on the calculation of confidence intervals when estimating parameters using various methods, deterministic or probabilistic. Here, as an example, we present the method of edgehog extremal solutions [24, 23, 27, 36].

The edgehog extremal solutions are those which correspond to parameters $p_0 + \delta p$ satisfying

$$J = \sigma_1^2, \| \delta p \|^2 \leq \sigma_2^2 \quad \text{or} \quad J \leq \sigma_1^2, \| \delta p \|^2 = \sigma_2^2$$

for given σ_1^2, σ_2^2. σ_1^2 is the admissible maximum residual which corresponds to the error in measurements, and σ_2^2 is the admissible maximum perturbation of the parameter.

Assume that the matrix of weights is of the form $W = wI$ with $w \in \mathbb{R}$ and I the identity matrix, and introduce the residual of the linearized problem $r = \varphi'(p_0)\delta p - \delta z$. Then from equation (10) the error function J can be written as $J(\delta p) = wr^t r$.

We introduce also the SVD decomposition of the sensitivity matrix $A = \varphi\prime(p_0) = USV^t$. Notice that, when the matrix $W = wI$, the SVD decomposition of A is closely related to the

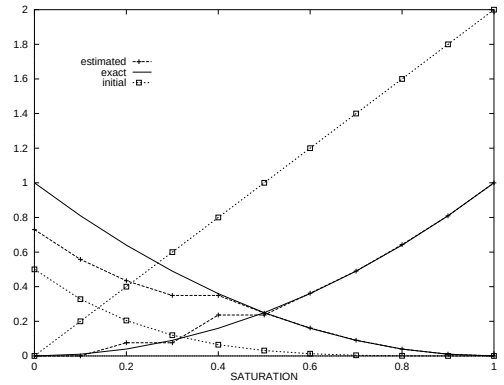

Relative permeabilities

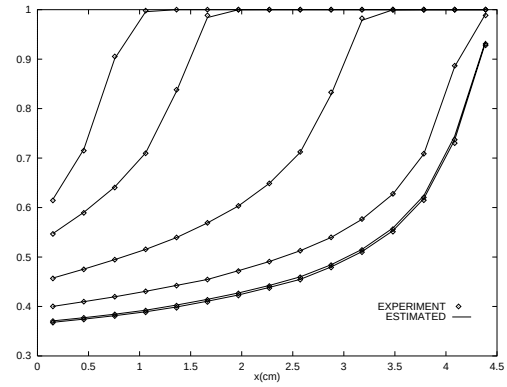

Saturation profiles

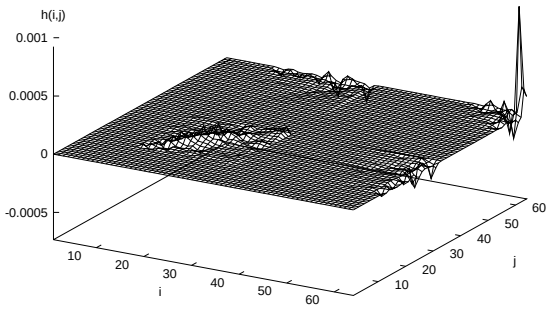

The Hessian H

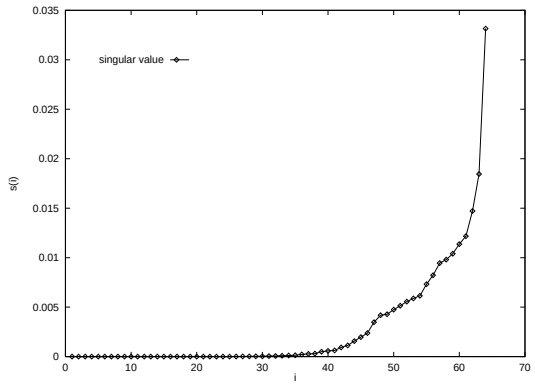

Singular Values

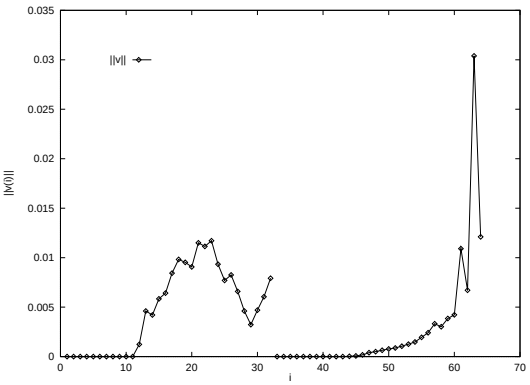

Sensitivity of saturation profiles

Figure 4: Problem 1 : Estimating relative permeabilities while measuring saturation profiles

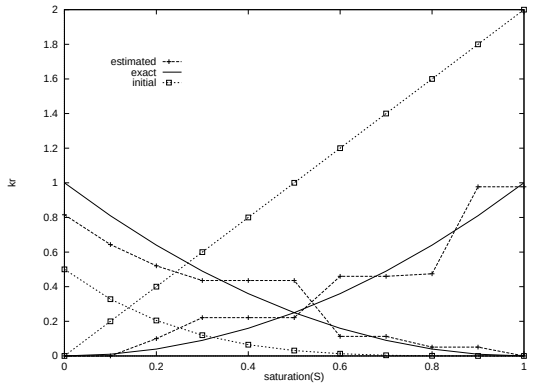

Relative permeabilities

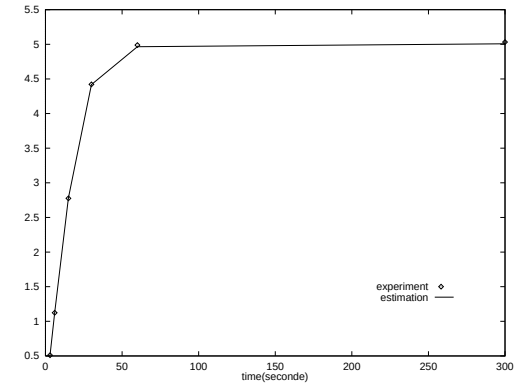

Productions

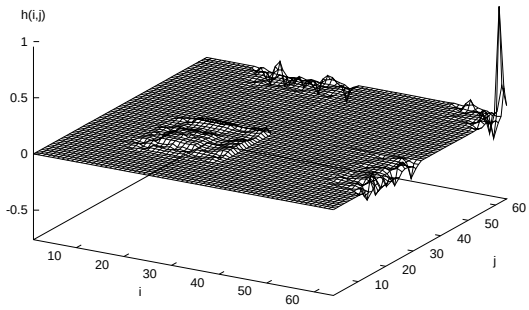

The Hessian H

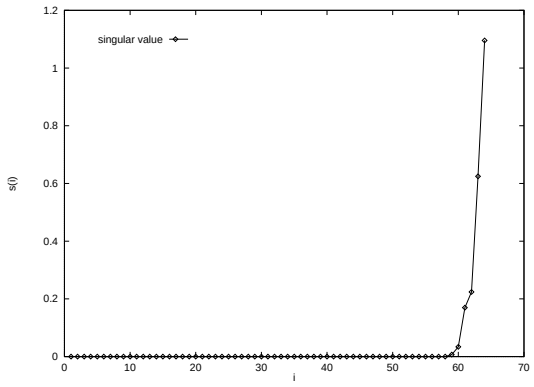

Singular Values

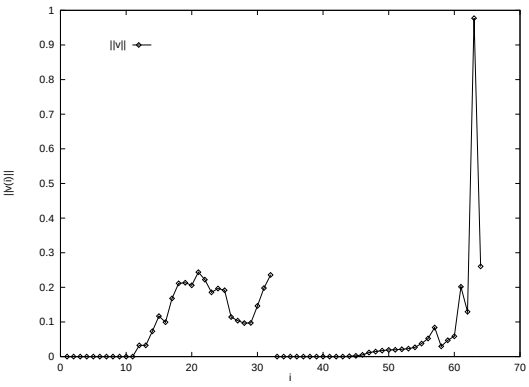

Sensitivity of saturation profiles

Figure 5: Problem 2 : Estimating relative permeabilities while measuring productions

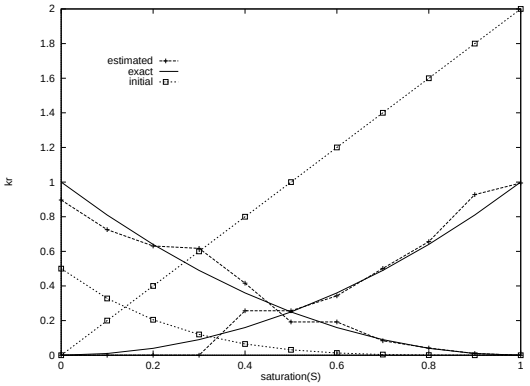

Relative permeabilities

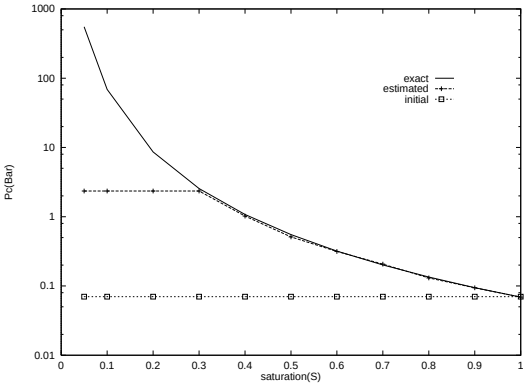

Capillary pressure

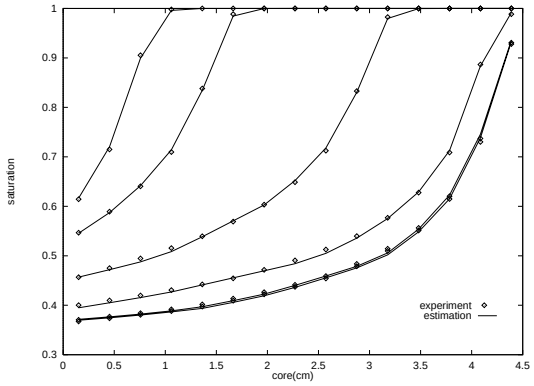

Saturation profiles

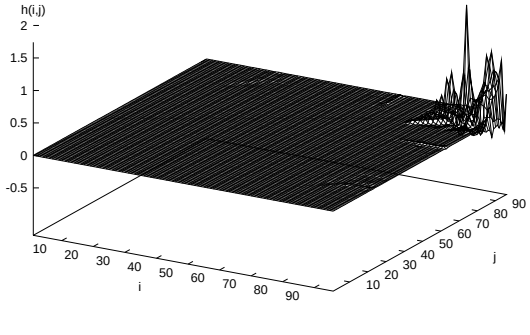

The Hessian H

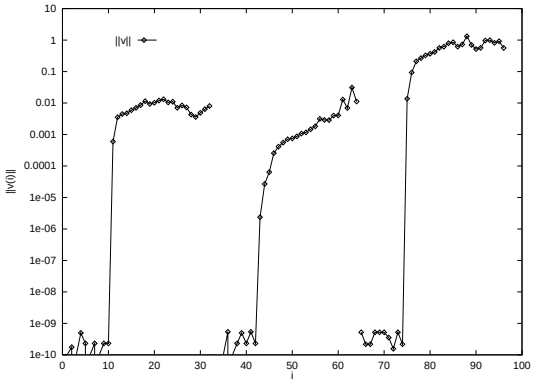

Sensitivity of saturation profiles

Figure 6: Problem 3 : Estimating relative permeabilities and capillary pressure while measuring saturation profiles

spectral decomposition of the Hessian H:

$$H = A^t W A = V S^t U^t W U S V^t = V \text{ diag } (w s_i^2) V^t = V \Lambda V^t$$

where the s_i's are the singular values of A and $\Lambda = \text{ diag } (\lambda_i) = \text{ diag } (w s_i^2)$.

Consider a perturbation δp parallel to the eigenvector V_k, $\delta p = a_k V_k$ and let us find the conditions it must satisfy in order to satisfy the edgehog conditions.

Then $J = w r^t r$ can be rewritten as $J = s_k^2 w a_k^2 - 2 s_k w \beta_k a_k + \hat{J}$ where β_k is the kth component of the vector $\delta z = z - \varphi(p_0)$ and $\hat{J} = \| \delta z \|_W^2 = \| \varphi(p_0) - z \|_W^2$. Therefore the edgehog condition $J = \sigma_1^2$ reduces to

$$s_k^2 w a_k^2 - 2 s_k w \beta_k a_k + \hat{J} - \sigma_1^2 = 0. \tag{12}$$

Solving for a_k we obtain $a_k = \dfrac{\beta_k}{s_k} \pm \dfrac{\sqrt{\beta_k + \sigma_1^2 - \hat{J}}}{\sqrt{\lambda_k}}$. Since p_0 is the calculated solution to the minimization problem, β_k is small and for s_k sufficiently large – which means that the sensitivity to the kth parameter is not too small – we obtain $a_k \approx \pm \dfrac{\sqrt{\sigma_1^2 - \hat{J}}}{\sqrt{\lambda_k}}$. Therefore we obtain the edgehog solution

$$p_E = p_0 + \delta p \approx p_0 \pm \frac{\sqrt{\sigma_1^2 - \hat{J}}}{\sqrt{\lambda_k}} V_k.$$

This implies that, as expected, the larger λ_k is, the smaller the uncertainty δp along V_k is.

When λ_k is small, the uncertainty δp becomes large and the edgehog condition $\| \delta p \|^2 = \sigma_2^2$ acts so $\delta p = \pm \sigma_2 V_k$. It remains to check that $J \leq \sigma_1^2$. Indeed it is easy to check that in this case a_k lies between the roots of the trinomial in the righthand side of equation (12).

Therefore the edgehog extremal solution associated to (λ_k, V_k) can be written as

$$p_E = p_0 + a_k V_k, \quad a_k = \pm \min\left(\frac{\sqrt{\sigma_1^2 - \hat{J}}}{\sqrt{\lambda_k}}, \sigma_2\right).$$

When H is diagonal a variation of the parameter δp in the direction of V_k corresponds to a variation of the kth parameter. When H is not diagonal, then the matrix H can be replaced by the diagonal matrices $\text{diag}(h_{ii})$ or $\text{diag}(\sum_j |h_{ij}|)$.

In a numerical experiment taken from [36] and whose results are shown in Fig. 7, H was replaced by $\text{diag}(\sum_j |h_{ij}|)$. The calculated minimum was $\hat{J} = 5.27 \times 10^{-6}$ since we were looking at the synthetic example. The data for calculating the edgehog extremal solutions were ${\sigma_1}^2 = 2.25 \times 10^{-3}$ which corresponds to an error of 0.005 on each saturation measurements, and $\sigma_2 = 2.4$ which corresponds to a bound of 0.3 on each parameter.

Again one can observe that for saturations smaller than 0.4 the confidence is small which is normal since during the experiment under study these values of the saturation are not reached. Actually we can observe that for values of the saturation smaller than 0.33 the extremal solution is determined by the edgehog condition $\sigma_2 = 2.4$.

7 A geometric approach to nonlinear stability analysis

In this section we recall results on nonlinear analysis for the problem of global minimization that were obtained by a geometric approach in several papers [9, 10, 8]. Actually in the following we will be in the case of a bounded admissible parameter set $\mathcal{A}$ in a finite dimensional parameter space $\mathcal{U}$. We will give sufficient conditions for the problem to have a unique global solution without local minima and give a stability result for the global solution. These results will be applied in the next section to the problem of estimating the relative permeabilities.

The following definition is devised to ensure both well-posedness and optimizability ???? of a nonlinear least square minimization problem.

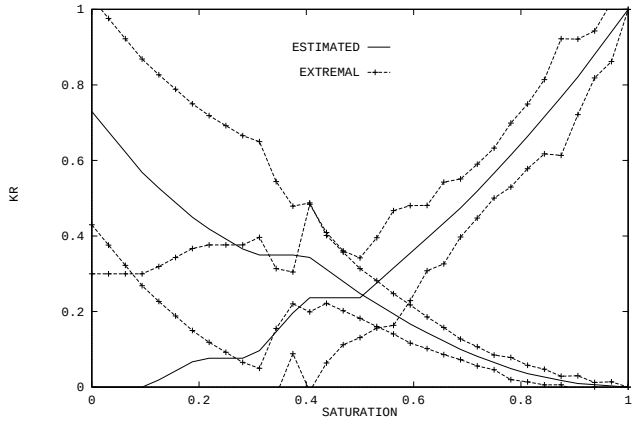

Figure 7: Estimated relative permeabilities with confidence intervals calculated with edgehog extremal solutions

Definition 1 *The nonlinear least square minimization problem (9),(8) is said to be Q-well posed if there exists $\mathcal{V}$, a neighborhood of $\varphi(\mathcal{A})$, and d, a distance on $\mathcal{A}$ such that, for all $z \in \mathcal{V}$*

1. *there exists a unique global minimum $\hat{p}$,*
2. *there is no local parasitic minima for the problem (9),(8),*
3. *the mapping $z \longrightarrow \hat{p}$ is Lipshitz continuous from $\mathcal{V} \subset \mathcal{O}$ to $\mathcal{A}$.*

In order to construct such a neighborhood $\mathcal{V}$ we introduce some notations. For any pair p_0, p_1 we associate a path Π in $\varphi(\mathcal{A})$ joining the points $\varphi(p_0)$ and $\varphi(p_1)$ which is the the image by φ of a straight path joining p_0 and p_1 in $\mathcal{A}$. We suppose that Π is twice differentiable with respect to its arclength s and we denote by $\Pi'(s)$ and $\Pi''(s)$ the velocity and the curvature vectors at $\Pi(s)$ (see Figure 8).

The length of the path Π defines a pseudo-distance on $\mathcal{A}$ between any two admissible parameters p_0 and p_1. We denote by $\delta(p_0, p_1)$ this pseudo-distance on $\mathcal{A}$.

Concerning curvature we introduce not only the usual radius of curvature

$$\rho(s) = \frac{1}{\| \Pi''(s) \|}$$

but also the global radius of curvature which is defined as follows [8]. Introduce N and N' the two affine subspaces normal to Π at the points $\Pi(s)$ and $\Pi(s')$, then the global radius of curvature $\rho_G(s, s')$ between the two points $\Pi(s)$ and $\Pi(s')$ is

$$\rho_G(s, s') = d(\Pi(s), N \cap N').$$

This quantity is not local since it depends not only on the curve at $\Pi(s)$ but also at $\Pi(s')$. Expressions for the global radius of curvature are given in Figure 9. One should note that

$$\rho_G(s, s') \neq \rho_G(s', s), \quad \lim_{s' \to s} \rho_G(s, s') = \rho(s).$$

We introduce now the set of maximum paths $\mathcal{P} = \{\Pi \mid p_0, p_1 \in \partial\mathcal{A}\}$, and we consider the worst case over one extremal path $\Pi \in \mathcal{P}$,

$$R(\Pi) = \inf_s \rho(s), \quad R_G(\Pi) = \inf_{s,s'} \rho_G(s, s'), \tag{13}$$

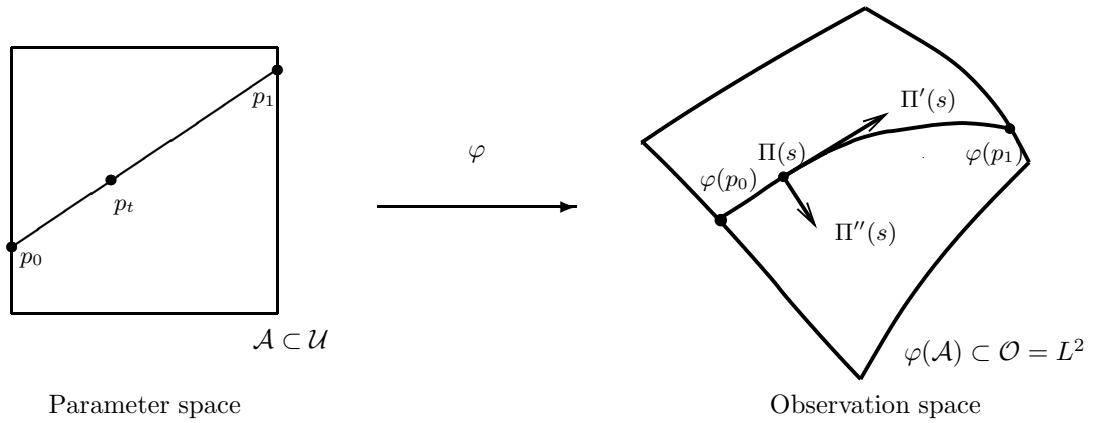

Figure 8: The direct mapping φ and a maximum path.

and for all maximum paths,

$$R = \inf_{\Pi \in \mathcal{P}} R, \quad R_G = \inf_{\Pi \in \mathcal{P}} R_G. \tag{14}$$

These numbers clearly satisfy $R_G(\Pi) \leq R(\Pi), R_G \leq R$.

Theorem 1 *Let $\mathcal{A}$ be bounded and $\mathcal{U}$ be finite dimensional. If $0 < R_G$, then the projection on $\varphi(\mathcal{A})$ is Q-well posed in the neighborhood $\mathcal{V} = \{z \,|\, d(z, \varphi(\mathcal{A})) < R_G\}$ of $\varphi(\mathcal{A})$ for the arc-length distance $\delta(p_0, p_1)$ on $\varphi(\mathcal{A})$. Furthermore the following estimates hold.*
If two measurements z_0 and z_1 are close enough so there exists a number d satisfying

$$\| z_0 - z_1 \| + \max_{j=0,1} d(z_j, \varphi(\mathcal{A})) \leq d < R_G, \tag{15}$$

then the following stability estimate holds for the corresponding parameters p_0, p_1 obtained by solving the associated least square problems :

$$\delta(p_0, p_1) \leq \frac{R(\Pi)}{R(\Pi) - d} \| z_0 - z_1 \|, \tag{16}$$

where Π is the path connecting $\varphi(p_0)$ and $\varphi(p_1)$.

Inequality (16) is a stability result for the arc length distance $\varphi(\mathcal{A})$. Depending on the hypothesis made on $\varphi\prime(p)$, it will imply two stability estimates on $\| p_0 - p_1 \|$ given below, the second one being sharper than the first one.

Q-well posedness:
Assume that

$$\text{There exists}\, \alpha_m > 0 \,\text{such that}\, \alpha_m \| q \| \leq \| \varphi'(p) q \| \;\text{ for all}\, p \in \mathcal{A}, q \in \mathcal{U}. \tag{17}$$

Then we have

$$\delta(p_0, p_1) = \int_0^1 \|\varphi'(p_0 + t(p_0 - p_1))(p_0 - p_1)\| dt \geq \alpha_m \| p_0 - p_1 \| .$$

Combining this inequality with estimate (16) we obtain

$$\| p_0 - p_1 \| \leq \frac{1}{\alpha_m} \frac{R}{R - d} \| z_0 - z_1 \|, \tag{18}$$

and problem (9),(8) is Q-well posed.

$L = sgn(s'-s) < \Pi(s') - \Pi(s), \Pi'(s') >$

Case I: $L \leq 0$

Then $\rho_G(s,s') = 0$.

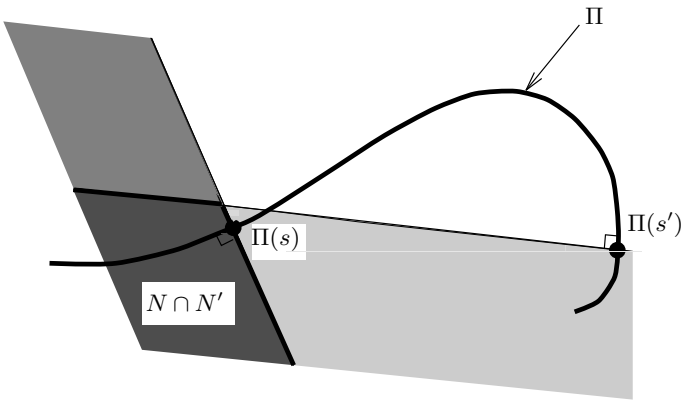

Case II: $L \leq 0$ and $< \Pi'(s), \Pi'(s') > \geq 0$

Then $\rho_G(s,s') = L$.

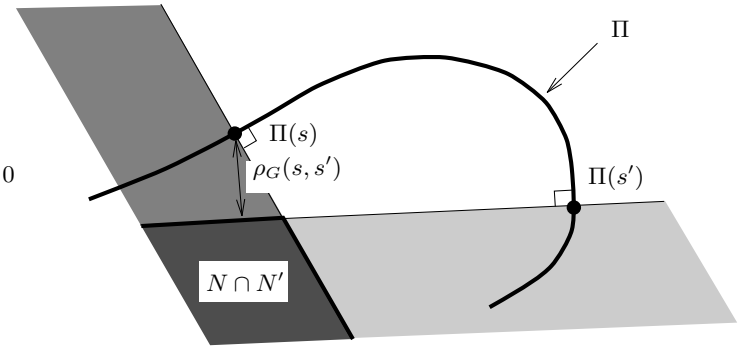

Case III: $L \leq 0$ and $< \Pi'(s), \Pi'(s') > \leq 0$

Then $\rho_G(s,s') = \dfrac{L}{\sqrt{1 - < \Pi'(s), \Pi'(s') >^2}}$

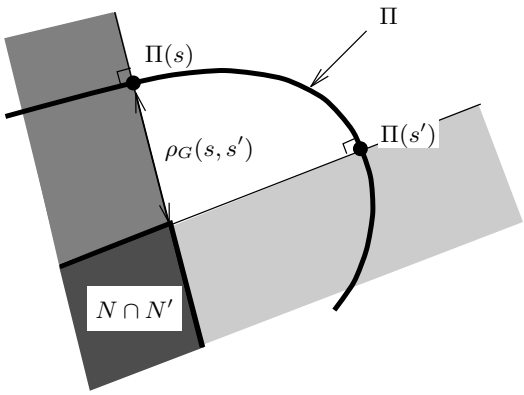

Figure 9: The global radius of curvature

Directional stability:
To improve the above estimate, we give now a directional estimate around a specific point, say p_0. We write $p_1 \in \mathcal{A}$ as $p_1 = p_0 + hv$ with $h = \| p_0 - p_1 \|$ and v a unit vector. We now assume, instead of (17):

$$\text{There exists } \overline{\alpha}_m(p_0, v) > 0 \text{ such that } \overline{\alpha}_m(p_0, v) \leq \| \varphi'(p_0 + tv)v \|, \text{ for all } p_0 + tv \in \mathcal{A}. \quad (19)$$

This is a less demanding condition than (17) since $\alpha_m \leq \overline{\alpha}_m(p_0, v)$. Then we have

$$\delta(p_0, p_1) = \int_0^1 \|\varphi'(p_0 + thv)hv\|dt \geq \overline{\alpha}_m(p_0, v)|h|.$$

Combining with (16) we obtain now

$$\| p_0 - p_1 \| = |h| \leq \frac{1}{\overline{\alpha}_m(p_0, p_1)} \frac{R(p_0, p_1)}{R(p_0, p_1) - d} \| z_0 - z_1 \| \quad (20)$$

where $R(p_0, p_1) = R(\Pi)$ is just a notation stressing the dependence of the smallest radius of curvature along Π between p_0 and p_1.

8 Implementation of the geometric nonlinear analysis

In this section we show how to use Theorem 1 in practice to estimate uncertainties in the parameters from uncertainties in the measurements. We consider a two-phase displacement where we estimate relative permeabilities of the form

$$kr_w(S) = S^a, \quad kr_{nw}(S) = (1 - S)^b.$$

Here a and b are the parameters to estimate. The constraints that we impose on them are $1 \leq a \leq 3, 1 \leq b \leq 3$ so $\mathcal{A} = (1, 3) \times (1, 3)$. The observations are saturation profiles. Saturations are measured at 6 different times in 5 different locations (30 measurements) in a first case, and in 15 different locations (90 measurements) in a second case. We set up the experiments so that we know the optimal parameters : $\hat{a} = \hat{b} = 2$.

To calculate estimates for R_G, R, α_m we proceed as follows :

1. Choose a sample of maximal paths $\mathcal{P}^*$ in $\mathcal{A}$ that we assume is large enough to represent $\mathcal{P}$ the set of maximal paths. An example is given in Fig. 8.

2. Discretize each paths with a set of points.

3. Calculate at these points Π, Π', Π'', these derivatives being made with respect to arc length and being calculated for instance by finite differences. Remember that each calculation of Π at one point requires a solution of the direct problem.

4. Calculate for each path $\Pi, R_G(\Pi), R(\Pi), \alpha_m(\Pi)$. For that we use equations (14) where we replace the infimum over all points of a path by that over the set of discretization points and the infimum over $\mathcal{P}$ by that over the subset $\mathcal{P}^*$ of $\mathcal{P}$. $\alpha_m(\Pi)$ is estimated by using finite differences with the points discretizing Π. The results are given in Table 1 for 30 measurements and for 90 measurements. From these results we obtain approximate values R_G^*, R^*, α_m^* of R_G, R, α_m for 30 measurements,

   $$R_G^* = R_G(AG) = 1.11 \times 10^{-3}, R^* = R(AG) = 1.11 \times 10^{-3}, \alpha_m^* = \alpha(BF) = 0.077,$$

   and for 90 measurements,

   $$R_G^* = R_G(EG) = 1.70 \times 10^{-2}, R^* R(EG) = 1.70 \times 10^{-2}, \alpha_m^* = \alpha(AG) = 0.28.$$

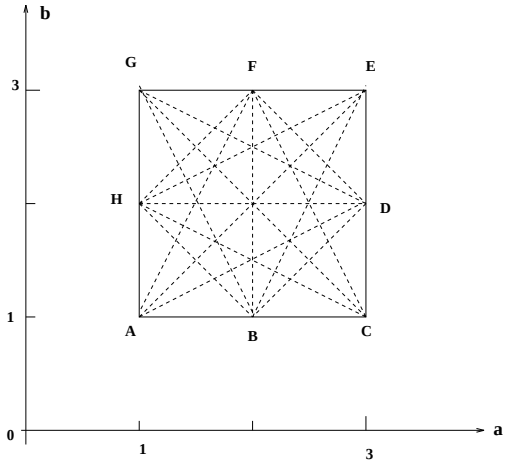

Figure 10: A sample of maximal paths for $\mathcal{A} = (1,3) \times (1,3)$.

Π	$R_G(\Pi)$	$R(\Pi)$	$\alpha_m(\Pi)$	$R_G(\Pi)$	$R(\Pi)$	$\alpha_m(\Pi)$
AC	2.34×10^{-2}	2.34×10^{-2}	0.267	6.44×10^{-2}	6.44×10^{-2}	0.545
AD	2.12×10^{-2}	2.12×10^{-2}	0.244	7.59×10^{-2}	7.59×10^{-2}	0.457
AE	1.71×10^{-2}	1.71×10^{-2}	0.205	4.95×10^{-2}	4.95×10^{-2}	0.392
AF	1.39×10^{-2}	1.39×10^{-2}	0.121	3.56×10^{-2}	3.57×10^{-2}	0.297
AG	$\mathbf{1.11 \times 10^{-3}}$	$\mathbf{1.11 \times 10^{-3}}$	0.520	3.07×10^{-2}	3.07×10^{-2}	**0.280**
BD	2.20×10^{-2}	2.20×10^{-2}	0.236	3.92×10^{-2}	3.92×10^{-2}	0.422
BE	9.46×10^{-3}	9.52×10^{-3}	0.140	2.70×10^{-2}	2.71×10^{-2}	0.360
BF	7.44×10^{-3}	7.44×10^{-3}	**0.077**	2.88×10^{-2}	2.88×10^{-2}	0.348
BG	2.75×10^{-3}	2.75×10^{-3}	0.138	2.68×10^{-2}	2.68×10^{-2}	0.375
BH	1.98×10^{-2}	1.98×10^{-2}	0.189	6.09×10^{-2}	6.09×10^{-2}	0.500
CE	4.90×10^{-3}	4.90×10^{-3}	0.085	2.92×10^{-2}	2.94×10^{-2}	0.414
CF	1.38×10^{-2}	1.39×10^{-2}	0.193	4.67×10^{-2}	4.67×10^{-2}	0.514
CG	4.01×10^{-3}	4.50×10^{-3}	0.190	2.20×10^{-2}	2.20×10^{-2}	0.421
CH	2.15×10^{-2}	2.15×10^{-2}	0.223	6.07×10^{-2}	6.07×10^{-2}	0.520
DF	1.92×10^{-2}	1.93×10^{-2}	0.266	6.04×10^{-2}	6.05×10^{-2}	0.606
DG	5.43×10^{-3}	5.91×10^{-3}	0.227	2.04×10^{-2}	2.09×10^{-2}	0.437
DH	1.78×10^{-2}	1.79×10^{-2}	0.236	6.28×10^{-2}	6.29×10^{-2}	0.476
EG	6.58×10^{-3}	6.58×10^{-3}	0.244	$\mathbf{1.70 \times 10^{-2}}$	$\mathbf{1.70 \times 10^{-2}}$	0.403
EH	2.61×10^{-2}	2.61×10^{-2}	0.202	4.17×10^{-2}	4.18×10^{-2}	0.365
FH	1.85×10^{-2}	1.85×10^{-2}	0.157	3.43×10^{-2}	3.43×10^{-2}	0.280
	30 measurements			90 measurements		

Table 1: Values of $R_G(\Pi), \alpha_m(\Pi), R(\Pi)$ for all paths $\Pi \in \mathcal{P}^*$ when using 30 and 90 measurements

	$\|\Delta S\|$	$\parallel \delta z \parallel$	$d = 2 \parallel \delta z \parallel$	$\parallel \delta p \parallel$
30 measur.	7.3×10^{-5}	0.0004	0.0008	0.0191
90 measur.	7.3×10^{-5}	0.0007	0.0014	0.0027

Table 2: Uniform estimates on the error δp on the parameter for a given error $|\Delta S|$ on a saturation measurement.

We can now apply Theorem 1.

Q-well posedness

In the case of 30 measurements, if the error on the measurements δz is such that

$$\parallel \delta z \parallel \leq R_G^* = 1.11 \times 10^{-3},$$

which corresponds to a 2×10^{-4} error on each saturation measurement, then it follows that the measurement z lies in the neighborhood $\mathcal{V}$. We see that (17) is satisfied with $\alpha_m = 0.077$ so that the nonlinear least square problem (8),(9) is Q-well posed.

Similarly, in the case of 90 measurements, if the error on the measurements δz is such that

$$\parallel \delta z \parallel \leq R_G^* = 1.7 \times 10^{-2},$$

which corresponds to a 1.8×10^{-3} error on each saturation measurement, then it follows that the measurement z lies in the neighborhood $\mathcal{V}$. We see that (17) is satisfied with $\alpha_m = 0.28$ so that the nonlinear least square problem (8),(9) is Q-well posed.

One can notice that, as expected, increasing the number of measurements allows for larger and larger errors on saturation measurements. Practically, even with 90 measurements, the precision required for the saturation measurements is difficult to achieve.

Stability

Given $p_0 = \hat{p}$ the estimated parameter, which is a minimizer of the nonlinear leat square problem (8),(9), we can use the stability result of theorem 1 to estimate the uncertainty δp in the following way. Denote $p_1 = p_0 + \delta p$ and assume that we know the uncertainty $|\Delta S| = 7.3 \times 10^{-5}$ on one saturation measurement. This uncertainty corresponds to an uncertainty $\parallel \delta z \parallel$ on the vector z of saturation measurements (see table 2). We take $d = 2 \parallel \delta z \parallel$ so that $d < R_G^*$ and hypothesis (15) is satisfied. Then inequality (18), when replacing R and α_m by R^* and α_m^* gives the uniform bounds on $\parallel \delta p \parallel$ given in table 2. These estimates on $\parallel \delta p \parallel$ can be represented by the domains of uncertainty shown in Fig. 11, circles centered at p_0 of radii $\parallel \delta p \parallel$. Note that these domains of uncertainty do not actually depend on the value of the optimal parameter p_0.

If, instead of inequality (18), we use inequality (20) to study the uncertainty with respect to saturation measurements, we proceed in the following way to build the domain of stability shown in Fig. 12 around the calculated minimum $p_0 = (2, 2)$. There are 6 paths of $\mathcal{P}^*$ going through p_0. On each of this path we look for the parameter p_1 the furthest from p_0 satisfying inequality (20). The domain of uncertainty is now an irregular polygon whose shape depends on p_0. Comparing the scales of Figs. 11 and 12, we observe that the domains of uncertainties obtained from 1st order directional estimate (20) are significantly smaller than those obtained from uniform estimate (18), confirming that estimate (20) is sharper than estimate (18).

We finally remark that in any case, having more measurements reduces the domains of uncertainty.

9 Conclusion

When estimating the relative permeability and capillary pressure functions in two-phase displacement experiments, we showed that much information about stability and uncertainty on the estimated parameters can be obtained from the Hessian.

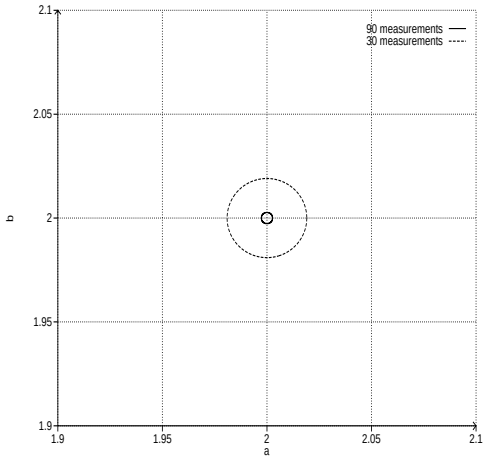

Figure 11: Domains of uncertainty from uniform estimate (18).

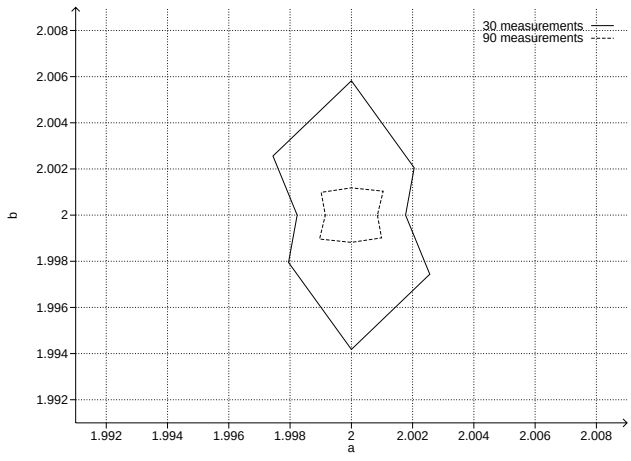

Figure 12: Domains of uncertainty from 1st order directional estimate (20).

Furthermore we showed also how to use in practice geometric nonlinear analysis tools to claim optimizability and to construct domains of uncertainty.

References

[1] S. Bitterlich and P. Knabner. An efficient method for solving an inverse problem for the richards equation. *Journal of Computational and Applied Mathematics*, 147:153–173, 2002.

[2] J.F. Bonnans, J.Ch. Gilbert, C. Lemaréchal, and C. Sagastizábal. *Numerical Optimization – Theoretical and Practical Aspects*. Springer Verlag, Berlin, 2003.

[3] C. Chardaire, G. Chavent, J. Jaffré, and J. Liu. Multiscale representation for simultaneous estimation of relative permeabilities and capillary pressure (paper SPE 20501). In *Proceedings of the 65th SPE Annual Technical Conference and Exhibition, New Orleans, Louisiana*. Society of Petroleum Engineers, Richardson, Texas, USA, 1990.

[4] C. Chardaire, G. Chavent, J. Jaffré, and J. Liu. Relative permeabilities and capillary pressure estimation through least square fitting. In P. King, editor, *The Mathematics of Oil Recovery*, pages 721–734. Clarendon Press, Oxford, 1992.

[5] C. Chardaire, G. Chavent, J. Jaffré, J. Liu, and B. Bourbiaux. Simultaneous estimation of relative permeabilities and capillary pressure. *SPE Formation Evaluation*, 7:283–289, 1992.

[6] C. Chardaire-Rivière, P. Forbe, J. Zhang, G. Chavent, and R. Lenormand. Improving the centrifuge technique by measuring local saturations, paper SPE 24882. In *proceedings of the 67th SPE Annual Technical Conference and Exhibition*, Washington, DC, U.S.A, October 1992. Society of Petroleum Engineers, Richardson, Texas, USA.

[7] G. Chavent. Identification of functional parameter in partial differential equations. In R.E. Goodson and M. Polis, editors, *Identification of Parameters in Distributed Systems*, pages 31–48. ASME, 1974.

[8] G. Chavent. New size $\times$ curvature condition for strict quasiconvexity of sets. *Siam J. Control and Optimization*, 29(6):1348–1372, 1991.

[9] G. Chavent. On the theory and practice of non-linear least-squares. *Adv. Water Resources*, 14(2):55–63, 1991.

[10] G. Chavent. Quasi-convex sets and size $\times$ curvature condition, application to nonlinear inversion. *Applied Mathematics and Optimization*, 24:129–169, 1991.

[11] G. Chavent, C. Chardaire-Rivière, and J. Zhang. Estimation of mobilities and capillary pressure from centrifuge experiments. In H.D. Bui et al., editor, *Inverse Problems in Engineering Mechanics*, pages 265–272. A.A. Balkema, Rotterdam, 1994.

[12] G. Chavent and G. Cohen. Numerical approximation and identification in a 1-d parabolic degenerated nonlinear diffusion and transport equation. In J. Stoer, editor, *Optimization techniques : Part 1*, volume 6 of *Lecture notes in Control and Information Sciences*, pages 282–293. Springer Verlag, Berlin, 1978.

[13] G. Chavent, G. Cohen, and M. Espy. Determination of relative permeabilities nad capillary pressure by an automatic adjustment method (paper SPE 9237). In *Proceedings of the 1980 SPE Annual Technical Conference and Exhibition, San Francisco*. Society of Petroleum Engineers, Richardson, Texas, USA, 1980.

[14] G. Chavent and J. Jaffré. *Mathematic Models and Mixed Finite Elements for Reservoir Simulation:single phase, multiphase and multicomponent flows trough porous media*. North-Holland, 1986.

[15] G. Chavent, J. Jaffré, and S. Jan-Jégou. Estimation of relative permeabilities in three-phase flow in porous media. *Inverse Problems*, 15:33–39, 1999.

[16] G. Chavent and P. Lemonnier. Identification de la non-linéarité d'une equation parabolique quasilinéaire. *Appli. Math. and Optim.*, 1(2), 1974.

[17] P. DuChateau. An inverse problem for the hydraulic properties of porous media. *SIAM J. Math. Anal.*, 28:611–632, 97.

[18] R.E. Ewing, M.S. Pilant, J.G. Wade, and A.T. Watson. Identification and control problems in petroleum and groudwater modeling. In I. Lasciecka and B. Morton, editors, *Control problems in industry*, volume 21 of *Progress in Systems and Control Theory*, pages 119–149. Birkhauser, San Diego, California, USA, 1995.

[19] A. Griewank. *Evaluating derivatives*. SIAM, 2000.

[20] A.-A. Grimstadt, K. Kolltveit, T. Mannseth, and J.-E. Nordvedt. Assessing the validity of a linearized accuracy measure for a nonlinear parameter estimation problem. *Inverse Problems*, 17:1373–1390, 2001.

[21] A.-A. Grimstadt and T. Mannseth. Nonlinearity, scale and sensitivity for parameter estimation problems. *SIAM J. Sci. Comput.*, 21:2096–2113, 2000.

[22] B. Igler and P. Knabner. Structural identification of nonlinear coefficient functions in transport processers though porous media. In H.J. Bungartz, R.H.W. Hoppe, and C. Zenger, editors, *Lectures on Applied Mathematics*, pages 157–178. Springer Verlag, Berlin, 2000.

[23] D.D. Jackson. Marginal solutions to quasi-linear inverse problems in geophysics: the edgehog method. *Geophys. J. R. astr. Soc.*, 35:121–136, 1973.

[24] D.D. Jackson. Most squares inversion. *J. of Geophysical Research*, 81(5):1027–1030, Februry 1976.

[25] S. Jégou. Using Maple for symbolic differentiation to solve inverse problems. *Maple Tech*, 4:32–40, 1997.

[26] P.D. Kerig and A.T. Watson. Relative permeability estimation from displacements experiments. *Society of Petroleum Engineers Res. Eng.*, pages 175–182, march 1986.

[27] Larry R. Lines and S. Treitel. Inversion with a grain of salt. *Geophysics*, 50(1):99–109, January 1985.

[28] G. Mejia, T. Watson, and J. Nordtvedt. Estimation of three-phase flow functions in porous media. *AIChE Journal*, 42:1957–1967, 1996.

[29] J.J. Moré. The Levenberg-Marquardt algorithm: implementation and theory. In G.A. Watson, editor, *Numerical Analysis*, number 630 in Lecture Notes in Mathematics, pages 105–116. Springer-Verlag, Berlin, 1978.

[30] G. Næval, T. Mannseth, K. Brusdal, and J.-E. Nordvedt. Multiscale estimation with spline wavelets, with applications to two-phase porous media flow. *Inverse Problems*, 16:315–332, 2000.

[31] J.E. Nordtvedt, G. Mejia, P.-H. Yang, and A.T. Watson. Estimation of capillary pressure and relative permeability functions from centrifuge experiments. *SPE Reservoir Engineering*, pages 292–298, November 1993.

[32] N.Z. Sun. *Inverse Problems in Groundwater Modeling*. Kluwer Academic Publishers, 1994.

[33] X.-C. Tai. Identification of a nonlinear parameter in a parabolic equation from a linear equation. *Comp. Appl. Mat.*, 14:157–184, 1995.

[34] O. Vignes. *Application of optimization methods in oil recovery problems.* PhD thesis, The Norwegian Institute of Technology, 1993.

[35] A.T. Watson, G.R. Gavalas, and J.H. Seinfeld. Identifiability of estimates of two-phase reservoir properties in history matching. *Society of Petroleum Engineers Journal*, pages 697–706, December 1984.

[36] J. Zhang. Sensibilité et stabilité dans l'estimation des perméabilités relatives et de la pression capillaire 'a partir de mesures de laboratoire. Thèse de Doctorat de l'Université Paris-Dauphine, 1994.

Centre de recherche INRIA Paris – Rocquencourt
Domaine de Voluceau - Rocquencourt - BP 105 - 78153 Le Chesnay Cedex (France)

Centre de recherche INRIA Bordeaux – Sud Ouest : Domaine Universitaire - 351, cours de la Libération - 33405 Talence Cedex
Centre de recherche INRIA Grenoble – Rhône-Alpes : 655, avenue de l'Europe - 38334 Montbonnot Saint-Ismier
Centre de recherche INRIA Lille – Nord Europe : Parc Scientifique de la Haute Borne - 40, avenue Halley - 59650 Villeneuve d'Ascq
Centre de recherche INRIA Nancy – Grand Est : LORIA, Technopôle de Nancy-Brabois - Campus scientifique
615, rue du Jardin Botanique - BP 101 - 54602 Villers-lès-Nancy Cedex
Centre de recherche INRIA Rennes – Bretagne Atlantique : IRISA, Campus universitaire de Beaulieu - 35042 Rennes Cedex
Centre de recherche INRIA Saclay – Île-de-France : Parc Orsay Université - ZAC des Vignes : 4, rue Jacques Monod - 91893 Orsay Cedex
Centre de recherche INRIA Sophia Antipolis – Méditerranée : 2004, route des Lucioles - BP 93 - 06902 Sophia Antipolis Cedex

Éditeur
INRIA - Domaine de Voluceau - Rocquencourt, BP 105 - 78153 Le Chesnay Cedex (France)
http://www.inria.fr
ISSN 0249-6399